ENERGETIC AND ECONOMIC OPTIMISATION OF A NOVEL HYBRID PV-THERMAL SYSTEM FOR DOMESTIC COMBINED HEATING AND POWER

María Herrando[1,2,*], James Freeman[1], Alba Ramos[1], Ignacio Zabalza[2], Christos N. Markides[1]
*Author for correspondence
[1]Clean Energy Processes (CEP) Laboratory, Department of Chemical Engineering, Imperial College London, London, UK
[2]University of Zaragoza-CIRCE Institute, Zaragoza, Spain
E-mail: maria.herrando11@imperial.ac.uk

ABSTRACT

Techno-economic performance calculations have been performed for a hybrid photovoltaic-thermal (PVT) collector design, featuring a novel polycarbonate flat-box absorber-exchanger configuration, integrated into a solar combined heat and power (S-CHP) system for the simultaneous provision of domestic hot water (DHW), space heating and power. The demands for electricity (including for lighting, cooling, and other home appliances), DHW and space heating from a single-family house located in two different climates, Zaragoza (Spain) and London (UK), were estimated and considered together with the local climate conditions in the S-CHP system performance analysis. The S-CHP system model used in this analysis includes the governing equations of the PVT unit, a hot-water storage tank, a water pump and a tank bypass. The capital (investment) cost of the system and the utility (electricity, natural gas) costs are also integrated into the model. The PVT array area and storage tank volume were sized to meet a minimum requirement for thermal energy demand coverage at each geographical location, and a seasonal optimisation of the collector flow-rate was performed to minimise the levelised production cost (LPC) of electrical and thermal energy and the levelised emissions displacement cost (LEDC). The results show that the S-CHP system optimised for Zaragoza with an array of 14 PVT collectors (covering 22 m^2, with a 3.4-kW_e peak electrical power rating) can provide 77% of the total household thermal demand and 145% of its electrical demand, averaged over the four seasons, with the surplus electricity exported to the grid, generating additional income. With the system optimised for London and an array of 17 PVT collectors (covering 26 m^2, with a 4.1-kW_e peak electrical power rating), the system provides 55% and 153% of the household thermal and electrical demands, respectively.

INTRODUCTION

A hybrid photovoltaic-thermal (PVT) collector is a solar energy collector consisting of a PV module in contact with a thermal absorber that is capable of generating both electrical and thermal outputs from the same collector area. Similarly to conventional PV and solar-thermal systems, PVT systems have the added benefit of moving energy generation closer to the point of use, and hence reducing the demands on the costly energy distribution infrastructure. This makes these systems particularly promising for domestic applications.

The most widely studied absorber-exchanger configuration in PVT collectors is that of parallel copper tubes (sheet-and-tube) with water or water-glycol mixtures as the heat transfer fluid [1–6], which is also the one used most commonly in commercially-available PVT panels. In this configuration, the amount of heat that can be extracted, and thus the overall efficiency that can be achieved, depends upon the collector fin efficiency and the tube bonding quality [7]. Consequently, several authors have made significant efforts to optimise the design of these collectors by paying attention to these design aspects [4,5], while others have proposed a flat-box structure with square or rectangular channels in order to significantly increase the heat transfer area between the absorber plate and the cooling fluid [1,7–12]. Some of these studies [1,7,12] have considered extruded aluminium alloy as the absorber-exchanger material; while in others [8,10,11], polycarbonate (PC) is proposed in order to lower the cost and weight of the PVT unit.

The work presented in this paper focuses on the techno-economic performance optimisation of a PC flat-box PVT panel for solar combined heat and power (S-CHP) provision in a domestic application. Previous research undertaken by the authors [13] indicated that with this absorber-exchanger configuration, improved heat transfer and higher efficiencies can be achieved. Specifically, 4% higher optical efficiency and about 15% lower heat loss coefficient were estimated, leading also to a 9% reduction in weight and a 21% reduction in investment cost compared to a commercial PVT system based on a copper sheet-and-tube arrangement.

METHODOLOGY

A quasi-steady state model of the complete solar combined heat and power (S-CHP) system has been developed in the software EES [14] with which to assess the techno-economic performance of the novel absorber-exchanger PVT collector configuration proposed in this research. The model has been used to simulate the system's performance over a typical week in each season (winter, spring, summer and autumn). From these simulations, important S-CHP system component parameters, specifically: the number of PVT panels, the required volume of the hot-water storage tank, and the PVT collector flow-rate, have been assessed and optimised.

S-CHP PVT system model

In Fig. 1, a section of the PVT collector considered in the present work together with the main heat transfer mechanisms are shown. The PVT panel has a nominal electrical power rating of 240 W_P and a total aperture area of 1.55 m^2 [13]. The S-CHP model contains the governing equations of the PVT collector based on the ASHRAE method [15], which includes parameters describing the PVT geometry (such as fin efficiency F, heat removal factor F_R, overall heat loss coefficient U_L, etc.), adapted to the flat-box structure. The full set of equations in the PVT model developed by the authors can be found in Ref. [2]. The two main components of the PVT panel are the PV module and thermal collector, which can be further divided into the glazing, the thermal absorber and the riser tubes (referred to as the absorber-exchanger unit), and the insulation layer (see Fig. 1). Similarly to other PVT modelling attempts [4,16], energy balances are written in order to evaluate the heat fluxes and temperatures in the collector. The equations are applied separately to each layer of the PVT collector, instead of using global equations to find the average absorber plate temperature and energy flows [17,18]. This allows an estimation of the average temperatures of all the separate unit layers [2].

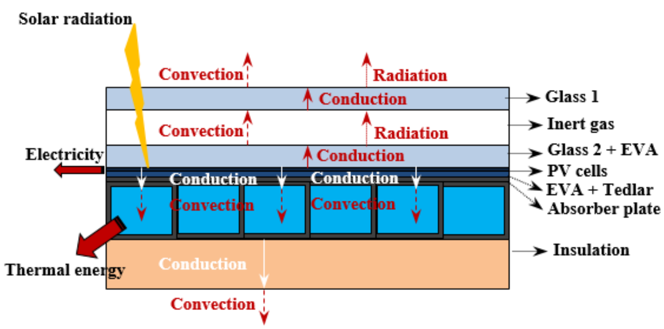

Figure 1 PVT collector cross-section for the flat-box structure configuration.

The S-CHP system model developed in this work for the provision of domestic hot water (DHW), space heating and power is shown in Fig. 2. It comprises an active closed-loop system in which, in normal operation, the collector outlet flow enters the heat exchanger coil located inside the storage tank, heats the water in the tank, exits the tank and returns to the inlet of the solar collector to be heated again. The hot-water storage tank is modelled using a 1-D stratified-tank model with 6 nodes. In the sizing calculation, the storage tank volume is varied within the range $50 < V_t/A_c < 180$ [19], where V_t is the tank volume in litres and A_c is the total PVT collector area.

A bypass valve is required to control the temperature of the cooling fluid leaving the collector and entering the tank, to ensure that this stream only heats (and does not cool) the water in the tank. This valve is controlled so that collector fluid is sent to the heat exchanger coil only when the outlet flow temperature from the collector is greater than that of the water in the storage tank. If this is not the case, the fluid is returned to the collector via the bypass connection for further heating.

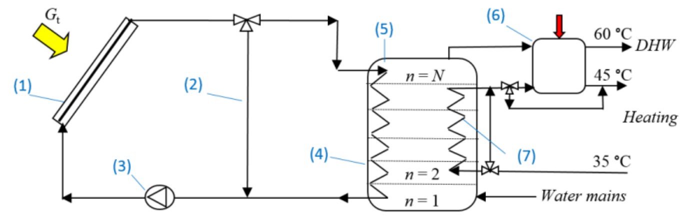

Figure 2 Schematic diagram of the S-CHP PVT system: (1) PVT collector, (2) PVT by-pass, (3) circulator pump, (4) PVT-tank heat exchanger coil, (5) stratified storage tank, (6) auxiliary heater, (7) space heating-tank heat exchanger coil.

The size of the solar heat exchanger coil also varies with the tank size such that the ratio between the coil heat transfer area and the total PVT collector area (A_c) is not lower than 0.15 [20] to ensure adequate heat transfer. To provide space heating (via radiant underfloor heating, UFH) to the household, a second heat exchanger coil is located in the tank (see Fig. 2). Water flowing in a separate closed-loop circuit enters the heat exchanger coil at the UFH return temperature of 35 °C and is heated to a target supply temperature of 45 °C. Again a bypass is included, to avoid sending fluid to the heat exchanger when the tank temperature is lower than 35 °C. As shown in Fig. 2, DHW is provided from an outlet port at the top of the tank, where a (gas-fired) auxiliary heater (nominal efficiency of 88% [2]) is located to raise the temperature up to a (fixed) supply temperature of 60 °C when required.

Reference single-family house

To simulate the performance of the S-CHP system for a domestic application, a reference house (semi-detached with 2 floors with an area of ~55 m^2 each, U-value of the façade 0.35 W/(m^2 K), double-glazed windows) has been modelled in EnergyPlus [21] to estimate the energy demand throughout the different seasons, including electricity for lighting, cooling and other household appliances, and natural gas for space heating and DHW. Typical occupancy profiles of a 4-inhabitant house (2 adults, 2 children) are considered, including lighting, HVAC and home appliances usage schedules, and temperature set-points of 21 °C for space heating and 26 °C for air conditioning are set. The estimated domestic energy demand varies across different geographical locations, and the locations chosen for the present study are Zaragoza (Spain) and London (UK). The estimated annual electricity and thermal demands are 47.4 kWh/m^2 and 95.5 kWh/m^2, respectively for Zaragoza, and 37.9 kWh/m^2 and 159.3 kWh/m^2 for London.

The half-hourly demand values are provided as inputs to the S-CHP model together with climate conditions for the specific locations. Among the outputs calculated by the model at each half-hourly time-step are the temperatures of the different layers of the PVT collector, the collector water outlet temperature, the water temperatures at each node of the storage tank, the electrical and thermal energy generated by the complete system and the percentages of demand covered.

Economic Assessment

In order to optimise the S-CHP system installation's size and operating conditions, the levelised production cost (LPC) and the levelised emissions displacement cost (LEDC) are estimated. To this end, the capital (investment) cost and the operation and maintenance (O&M) costs of the system are considered, as well as the utility (electricity, natural gas) costs that are incurred to satisfy the rest of the electrical and thermal demand of the household that cannot be covered by the system.

The system's investment cost is estimated from price lists available from solar retailers in the EU. The main costs of system are associated with the storage tank, the PVT collectors, the circulating fluid, the pump station (consisting of a circulator pump, the electronic controller and the temperature sensors) and the piping and fixings. The costs of the electrical installation are taken from price lists for roof mounted PV kits (excluding the cost of the PV module) [22]. The cost of the storage tank is estimated using a correlation based on market prices of existing tanks across a range of storage volumes. The total installation costs are also considered [23].

In order to consider the time value of money, a discounted cash flow analysis is undertaken to estimate the net present value (NPV) of the complete system, as follows,

$$NPV = C_0 + A_i \cdot \left[\frac{(1+r)^n - 1}{r \cdot (1+r)^n} \right] \tag{1}$$

where C_0 is the total investment cost of system, r is the discount rate, estimated as 8% in this work, n is the system's lifetime (assumed to be 25 years) and A_i is the total annual running costs incurred, which are the sum of the running costs due to the electricity (C_e) and natural-gas (C_{aux}) that should be bought from the grid to completely cover the household's energy demand, as well as the O&M costs of the system ($C_{O\&M}$),

$$A_i = C_e + C_{aux} + C_{O\&M} \tag{2}$$

Actual electricity and natural-gas prices for domestic consumers in both locations, London (UK) and Zaragoza (Spain) are used to calculate the running costs [24–26]. The present-day feed-in-tariffs (FITs) available in the UK are also included [27], and applied for both locations to compare the results, even though no FITs are currently available in Spain.

The NPV is annualised to estimate the levelised cost (L),

$$L = NPV \cdot \left[\frac{r \cdot (1+r)^n}{(1+r)^n - 1} \right] \tag{3}$$

which is used to calculate the LPC and LEDC,

$$LPC = \frac{L\,(€/year)}{Final\,Energy\,Output\,(kWh/year)} \tag{4}$$

$$LEDC = \frac{L\,(€/year)}{Emissions Displaced\,(kg\,CO_2/year)} \tag{5}$$

Conversion factors to CO_2 emissions specific to each location are used to obtain the annual displaced emissions [28,29].

RESULTS AND DISCUSSION

In this section, results from the system evaluation are presented. Firstly, the techno-economic performance of the proposed S-CHP system is assessed over a week in each season, with the aim of selecting the most appropriate installation size (number of PVT panels and storage tank volume) for a single-family house in the respective locations of London and Zaragoza. With the sizing parameters fixed, a seasonal optimisation is undertaken to estimate the optimum collector flow-rate that leads to the lowest LPC and LEDC in each case. Finally, performance profiles for selected days with the optimised configuration are presented and discussed.

Techno-economic assessment

The objective of the sizing exercise is to determine a suitable size for the S-CHP system in order to provide a minimum fraction of the household energy demand. A minimum of 40% of the thermal (space heating plus DHW) demand is chosen for the present analysis. To this end, the number of PVT collectors is varied up to 26 (varying the tank dimensions accordingly), which corresponds to a total PVT array area of 40 m^2 and the maximum useable roof area on the single family dwelling-type chosen for this study. The flow-rate through each PVT collector (V_p) is fixed in this analysis to 50 L/h. The PVT collectors are connected in parallel so that the total flow-rate through the array is equal to the individual collector flow-rate multiplied by the number of collectors.

The results for Zaragoza, presented in Table 1, show that with 14 PVT collectors (covering 22 m^2, with a 3.4 kW$_e$ peak electrical power rating) and a 2.0-m^3 hot-water storage tank (V_t/A_c = 90.6), it is possible to cover 41% of the total thermal demand in winter, and more than 85% in the rest of the seasons. Furthermore, in all seasons except summer there is a surplus of electricity that can be sold to the grid. Averaged over the four seasons, a thermal-demand coverage of 77% and an electrical demand coverage of 145% is achieved.

Table 1 Percentage of thermal and electrical demands covered, LPC and LEDC with a S-CHP system consisting of 14 PVT collectors installed in a single-family house in Zaragoza.

	Thermal demand (%)	**Electrical demand (%)**	**LPC (€/kWh)**	**LEDC (€/kgCO$_2$)**
Winter	41	162	0.18	0.57
Summer	90	72	0.31	0.92
Spring	86	158	0.21	0.64
Autumn	90	187	0.19	0.58
Average	*77*	*145*	*0.23*	*0.68*

In the case of London, 17 PVT collectors (covering 26 m^2, with a 4.1 kW$_e$ peak electrical power rating) and a 2.4-m^3 hot-water storage tank (V_t/A_c = 90.6) are required to cover the minimum thermal-demand fraction in all four seasons. As shown in Table 2, the demand coverage averaged over all of the seasons is 55% (thermal) and 153% (electrical), again resulting in a surplus of electricity that can be sold to the grid.

Table 2 Percentage of thermal and electrical demands covered, LPC and LEDC with a S-CHP system consisting of 17 PVT collectors installed in a single-family house in London.

	Thermal demand (%)	Electrical demand (%)	LPC (€/kWh)	LEDC (€/kgCO_2)
Winter	41	166	0.18	0.65
Summer	89	132	0.27	0.75
Spring	49	185	0.18	0.59
Autumn	40	130	0.24	0.85
Average	*55*	*153*	*0.22*	*0.71*

S-CHP PVT system seasonal optimisation

Once the S-CHP system size is selected for each location, the flow-rate per PVT collector (V_p) is optimised seasonally to obtain the lowest LPC (€/kWh) and the lowest LEDC (€/kg CO_2 displaced). To this end, V_p is allowed to vary in the range from a minimum of 5 L/h to a maximum of 200 L/h.

In the case of Zaragoza, the results show that the minimum LPC and LEDC are achieved at different collector flow-rates in each season, requiring low flow-rates in winter and spring, and high flow-rates in summer and autumn (see Table 3). It is also possible to observe that very similar values of LPC and LEDC are obtained whether the optimisation is set to minimise LPC (first 3 columns in Table 3) or to minimise LEDC (last 3 columns in Table 3), although the difference in the optimal flow-rates obtained for the two objective functions is not significant. Therefore of the two optimal flow-rate values obtained for each season, the lower flow-rate is recommended as it would lead to a lower pumping energy consumption.

Within the range of flow-rates considered (V_p = 5-200 L/h per collector), the covered thermal-energy demand varies from 28% to 43% in winter and from 79% to 96% in summer, while the electrical demand covered varies from 135% to 167% in winter and from 68% to 73% in summer.

Table 3 Optimal flow-rates per PVT collector (V_p) for each season that minimise the LPC and LEDC for a S-CHP system comprising 14 PVT collectors installed in a single-family house in Zaragoza (Spain).

	Minimise LPC (€/kWh)			Minimise LEDC (€/kgCO_2)		
	LPC	V_p (L/h)	**LEDC**	**LEDC**	V_p (L/h)	**LPC**
Winter	0.17	26	0.56	0.56	27	0.17
Summer	0.31	133	0.91	0.91	150	0.31
Spring	0.21	16	0.64	0.64	24	0.21
Autumn	0.19	148	0.57	0.56	200	0.19

For London, the result of choosing LPC or LEDC as the objective function of the optimisation results in a considerable difference in the optimal flow-rate in summer, but only a small difference in the corresponding values of LPC and LEDC (less than 1%) (see Table 4). For the rest of the seasons, the same optimal flow-rates are found irrespective whether the optimisation is set to minimise LPC or LEDC. Comparing Table 4 to Table 3, optimal flow-rates are found to be lower for London than for Zaragoza in summer and autumn, while for winter and spring, optimal flow-rates are higher. This is attributed to the higher irradiance levels and ambient temperatures in Zaragoza in summer and spring, so higher flow-rates are required to avoid overheating.

In this case, the thermal energy demand covered varies from 20% to 42% in winter and from 69% to 97% in summer, while the electrical demand covered varies from 120% to 172% in winter and from 124% to 134% in summer (within the range of flow-rates considered (V_p = 5-200 L/h per collector)).

Table 4 Optimal flow-rates per PVT collector (V_p) for each season that minimise the LPC and LEDC for a S-CHP PVT system comprising 17 PVT collectors installed in a single-family house in London (UK).

	Minimise LPC (€/kWh)			Minimise LEDC (€/kgCO_2)		
	LPC	V_p (L/h)	**LEDC**	**LEDC**	V_p (L/h)	**LPC**
Winter	0.17	38	0.64	0.64	39	0.17
Summer	0.27	23	0.75	0.74	85	0.27
Spring	0.17	40	0.59	0.59	40	0.17
Autumn	0.24	31	0.83	0.83	31	0.24

Daily Analysis

Half-hourly results concerning the electrical performance of the S-CHP system over the last three consecutive days of the spring week are shown in Figs. 3 and 4 for Zaragoza (Spain) and London (UK), respectively. In these plots, negative values of net electricity (green crosses) mean that the household electricity-demand cannot be covered at that time-instant by the PVT generation so the deficit should be bought from the grid. On the contrary, positive values of net electricity mean that there is a surplus, which can be sold to the grid.

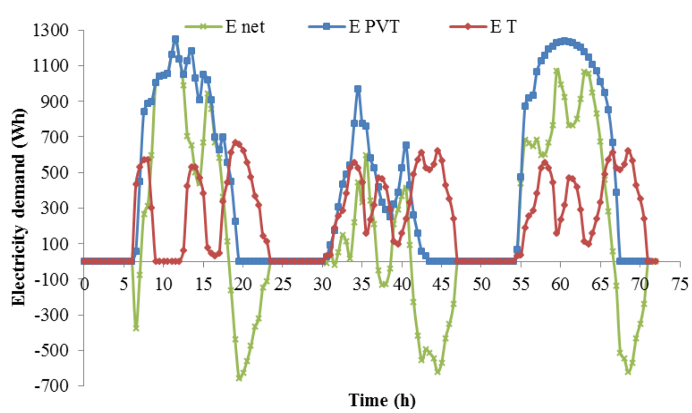

Figure 3 Total household electricity demand (E_T), net electricity (E_{net}) demand and electricity generated (E_{PVT}) by the optimised S-CHP PVT system over three consecutive spring days in Zaragoza (Spain).

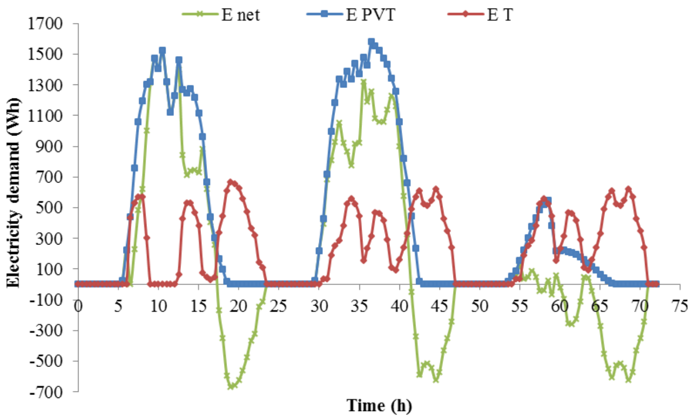

Figure 4 Total household electricity demand (E_T), net electricity (E_{net}) demand and electricity generated (E_{PVT}) by the optimised S-CHP PVT system in a three consecutive spring days in London (UK).

In these figures, it is possible to observe the differences in the performance and operation of the system between cloudy and sunny days. It is also interesting to see that there is a mismatch between the peak electricity demand and the peak electricity generation, so some mechanism (e.g. storage) is ideally required to shift these curves. In this case, the flexibility of buying/selling electricity from/to the grid through the electricity price/FIT is considered, but other options such as the use of batteries could be assessed, which would also be the only available solution to isolated households.

Figures 5 and 6 show half-hourly results concerning the thermal performance of the S-CHP system over the same three days used in Figs. 3 and 4 for Zaragoza (Spain) and London (UK), respectively. The results indicate that on the selected (spring) days, almost the entire thermal (DHW plus space heating) demand is covered by the S-CHP system in Zaragoza. On the other hand, the system in London can only cover the full thermal demand over the first two days (characterised by high irradiance); on the third day a much smaller fraction of demand is met due to the low irradiance. This also results in a lower electrical-demand coverage, shown for the final day in Fig. 4.

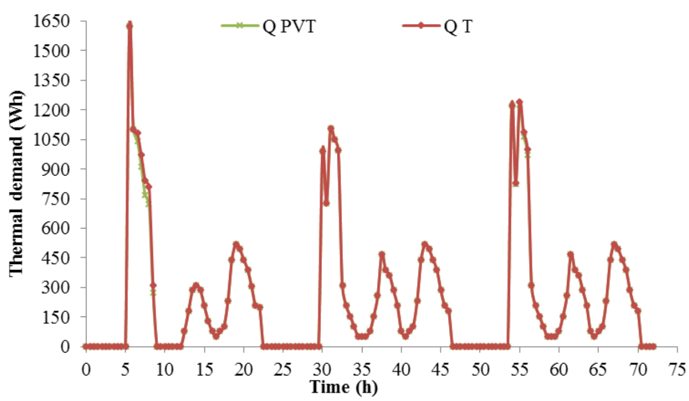

Figure 5 Total household thermal (space heating plus DHW) demand (Q_T) and thermal demand covered (Q_{PVT}) by the optimised S-CHP PVT system in a three consecutive spring days in Zaragoza (Spain).

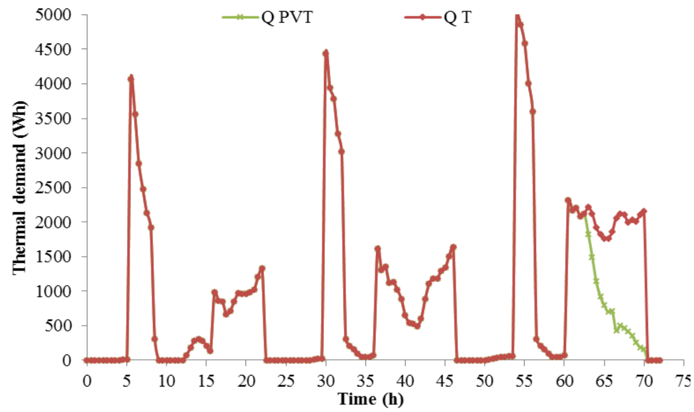

Figure 6 Total household thermal (space heating plus DHW) demand (Q_T) and thermal demand covered (Q_{PVT}) by the optimised S-CHP PVT system in a three consecutive spring days in London (UK).

From these results it can be concluded that the geographical location and climate have a significant effect on the performance and cost-effectiveness of the S-CHP system, with low irradiance conditions resulting in a higher demand for auxiliary energy and thus higher fuel costs, and also lower additional revenues from exporting surplus electricity. Specifically, the results show that higher latitude and colder locations, such as London (UK), require more collector area and in general lower collector flow-rates to cover the same energy demand compared to lower latitude and warmer locations, such as Zaragoza (Spain). Lower ambient temperatures in the UK also lead to higher thermal energy (specifically space heating) demands and lower S-CHP system thermal outputs.

CONCLUSIONS

A promising new flat-plate hybrid photovoltaic-thermal (PVT) collector configuration based on a polycarbonate (PC) flax-box structure was assessed from a techno-economic perspective. To this end, a 1-D model of the PVT collector was integrated into a complete solar combined heat and power (S-CHP) system model, including a 1-D stratified hot-water storage tank model. The energy demands of single-family houses located in two different locations, Zaragoza (Spain) and London (UK), were modelled in EnergyPlus. The model was run on a half-hourly basis for a whole week and the system parameters were assessed and optimised for each season.

The results show that, in order to cover at least 40% of the thermal (space heating plus DHW) demand of a single-family house in any season, a S-CHP system with 14 PVT collectors (covering 22 m^2, with a 3.4-kW$_e$ peak electrical power rating) is required in Zaragoza, and one with 17 PVT collectors (covering 26 m^2, with a 4.1-kW$_e$ peak electrical power rating) is required in London. With these installation sizes, it is expected that the annual electricity generated in both climates will be more than the annual demand (including lighting, cooling, and other home appliances), however, an auxiliary electricity supply is still required due to the mismatch between the times of supply and demand, while surplus electricity during times of over-supply may be sold to the grid to earn additional revenue. The novel flax-box PVT configuration considered in this work is expected to achieve better results in terms of energy demand coverage and system cost-effectiveness compared to commercial copper sheet-and-tube PVT panels, due to the energy performance enhancement and lower investment cost of the former. A detailed analysis is being undertaken in this line.

In terms of performance optimisation, the results show that to minimise the cost per kWh (LPC) and the cost per kg of CO_2 emissions displaced (LEDC), the optimum collector flow-rate varies with the season in the case of Zaragoza, with high flow-rates (133-148 L/h) preferred in summer and autumn, and low flow-rates (16-26 L/h) preferred in winter and spring. In London on the other hand, moderately low flow-rates (23-40 L/h) are optimal in all seasons. Therefore, it can be concluded that, in some climates (especially low-latitude warmer locations such as Zaragoza), it may be beneficial to install a variable-speed pump or to manually change the collector flow-rate on a seasonal basis so as to improve the performance of such a system, while in other climates characterised by lower irradiance levels such as the UK, seasonal variations to the flow-rate do not lead to a significant benefit in terms of reducing the levelised cost of the system.

REFERENCES

[1] Chow TT, Ji J, He W. Photovoltaic-Thermal Collector System for Domestic Application. *J Sol Energy Eng*, 2007;129:205.

[2] Herrando M, Markides CN, Hellgardt K. A UK-based assessment of hybrid PV and solar-thermal systems for domestic heating and power: System performance. *Appl Energy*, 2014;122:288–309.

[3] Tripanagnostopoulos Y, Souliotis M, Battisti R, Corrado A. Energy, cost and LCA results of PV and hybrid PV/T solar systems. *Prog Photovoltaics Res Appl*, 2005;13:235–50.

[4] Zondag HA, de Vries DW, van Helden WGJ, van Zolingen RJC, van Steenhoven AA. The yield of different combined PV-thermal collector designs. *Sol Energy*, 2003;74:253–69.

[5] Chow TT. Performance analysis of photovoltaic-thermal collector by explicit dynamic model. *Sol Energy*, 2003;75:143–52.

[6] Kalogirou SA. Use of TRNSYS for modelling and simulation of a hybrid pv–thermal solar system for Cyprus. *Renew Energy*, 2001;23:247–60.

[7] He W, Chow T, Ji J, Lu J, Pei G. Hybrid photovoltaic and thermal solar-collector designed for natural circulation of water. *Appl Energy*, 2006;83:199–210.

[8] Huang BJ, Lin TH, Hung WC, Sun FS. Performance evaluation of solar photovoltaic / thermal systems. *Sol Energy*, 2001;70:443–8.

[9] Shan F, Cao L, Fang G. Dynamic performances modeling of a photovoltaic-thermal collector with water heating in buildings. *Energy Build*, 2013;66:485–94.

[10] Cristofari C, Canaletti J, Notton G, Darras C. Innovative patented PV/TH Solar Collector: optimization and performance evaluation. *Energy Procedia*, 2012;14:235–40.

[11] Cristofari C, Notton G, Poggi P, Louche A. Modelling and performance of a copolymer solar water heating collector. *Sol Energy*, 2002;72:99–112.

[12] Chow TT, He W, Ji J. Hybrid photovoltaic-thermosyphon water heating system for residential application. *Sol Energy,* 2006;80:298–306.

[13] Herrando M, Guarracino I, del Amo A, Zabalza I, Markides CN. Energy Characterization and Optimization of New Heat Recovery Configurations in Hybrid PVT Systems. *ISES Conf. Proc.*, Palma de Mallorca (Spain), 2016.

[14] EES: Engineering Equation Solver | F-Chart Software : Engineering Software. http://www.fchart.com/ees/ (accessed April 7, 2017).

[15] ASHRAE Standard. Standard 93-2003. Methods of testing to determine the performance of solar collectors, 2013.

[16] Notton G, Cristofari C, Mattei M, Poggi P. Modelling of a double-glass photovoltaic module using finite differences. *Appl Therm Eng*, 2005;25:2854–77.

[17] Zondag HA, De Vries DW, Van Helden WGJ, Van Zolingen RJC, Van Steenhoven AA. The thermal and electrical yield of a PV-thermal collector. *Sol Energy*, 2002;72:113–28.

[18] Kalogirou SA. Solar thermal collectors and applications. *Prog Energy Combust Sci*, 2004;30:231–95.

[19] The Ministry of Housing of the Spanish Government. Section HE4 - Minimum Solar Domestic Hot Water contribution. *Building Technical Code, Basic Document Energy Savings*, 2013:1–129.

[20] IDAE and CENSOLAR. Solar Thermal Energy Installations. Technical Specifications Document of Low Temperature Installations, 2009.

[21] EnergyPlus software, https://energyplus.net/ (accessed February 9, 2017).

[22] Ramos A, Chatzopoulou MA, Guarracino I, Freeman J, Markides CN. Hybrid photovoltaic-thermal solar systems for combined heating, cooling and power provision in the urban environment. *Energy Convers Manag*, 2017.

[23] Herrando M, Markides CN. Hybrid PV and solar-thermal systems for domestic heat and power provision in the UK: Techno-economic considerations. *Appl Energy*, 2016;161:512–32.

[24] Spanish Ministry of Energy, Tourism and Digital Agenda (MINETAD). Net electricity price for domestic and industrial use, 2016.

[25] Energy Saving Trust. Average electricity and gas prices. http://www.energysavingtrust.org.uk/about-us/our-calculations (accessed March 27, 2017).

[26] The Spanish Ministry of Industry, Energy and Tourism. Regulated energy prices report, 2016.

[27] KPMG. UK solar beyond subsidy: the transition, 2015.

[28] UK Government. Greenhouse gas reporting - Conversion factors 2016. https://www.gov.uk/government/publications/greenhouse-gas-reporting-conversion-factors-2016 (accessed April 6, 2017).

[29] The Spanish Ministry of Industry Energy and Tourism. Conversion factors for CO_2 emissions and primary energy conversion for the different final energy sources in the building sector in Spain, 2016.